

Characteristics of “Dust” Fluxes from the Surface of Copper and Lead Liners Exposed to One or Two Successive Shock Waves

V. A. Ogorodnikov^a, S. V. Erunov^a, K. N. Panov^a, E. A. Chudakov^a, I. A. Blinov^a, *,
A. B. Georgievskaya^a, D. N. Zamyslov^a, and I. R. Farin^a

^a *Alekseev State Technical University of Nizhny Novgorod, Nizhny Novgorod, 603155 Russia*

**e-mail: postmaster@ifv.vniief.ru*

Received March 10, 2023; revised April 12, 2023; accepted April 18, 2023

Comparative experimental studies of the shock-induced particle ejection (“dusting”) from the free rough (Rz20) surface of copper and lead liners exposed to one or two successive shock waves separated in time by 0.2 μs have been carried out for the first time. This situation usually occurs in cumulative systems for the compression of the plasma by cylindrical or spherical liners shock or quasi-isentropically accelerated by explosion products. Using pulsed X-ray diffraction, laser optical recording, piezoelectric pressure sensors, and heterodyne interferometry, a qualitative picture has been studied and the quantitative characteristics of particle ejection from the free surface such as the velocities of the free surface and the particle flux front and the density (mass) distribution of particle flux in the direction of its motion, which are necessary for more accurate determination of features and the development of more appropriate models of the effect, have been evaluated.

DOI: 10.1134/S0021364023601203

1. INTRODUCTION

Shock-induced “dusting” in the physics of shock waves, i.e., particle ejection from the free surface of materials exposed to shock waves, has been quite actively studied in the last decade both theoretically and experimentally [1–24]. Data on the influence of the roughness of the surface, the amplitude of the shock wave, the phase state of a material, the presence of a gas in front of the free surface, and the pressure in the gas on dusting were obtained. Measures for the suppression of dusting were discussed.

However, in some schemes of the acceleration of liners by means of explosives, several shock waves are successively incident on the free surface. In this case, the picture of particle ejection from the free surface is noticeably complicated. On one hand, microroughnesses are partially removed after the action of the first shock wave on the free surface, and the free surface accelerated by the second shock wave can catch the particle flux from the first shock wave. On the other hand, the action of the second shock wave on the free surface can result, under certain conditions, in the formation of jet flows from regions between jets formed after the incidence of the first shock wave on the free surface. Furthermore, microdefects that can be formed in a liner under unloading after the incidence of the first shock wave on the free surface are additional sources of dusting for the second shock wave.

In this work, we report new results of the study of shock-induced dusting from the free surface of lead

and copper plate liners exposed to two successive shock waves separated in time by ~0.2 μs. The amplitudes of the first and second shock waves are 46 and 67 GPa for copper and 39 and 59 GPa for lead, respectively, which are insufficient for the melting of copper in the rarefaction wave and are sufficient for the melting of lead on the first shock wave [13, 19, 25].

The results obtained in this work are compared to the results from [23], where the qualitative picture and quantitative characteristics of shock-induced dusting from the free surface of similar copper and lead liners exposed to a single shock wave with approximately the same amplitudes of 50 and 45 GPa were studied. It is established and quantitatively confirmed for the first time that the incidence of the second shock wave on the free surface of the liner can noticeably affect the quantitative characteristics of shock-induced dusting for liners made of a material that does not melt under shock compression.

2. EXPERIMENTS

The schematic of experiments from [23] shown in Fig. 1a was also used in this work. To implement the two-shock loading, 2.0-mm-thick copper (M1) and 2.5-mm-thick lead (C1) plate liners 108 mm in diameter were separated by a 0.7-mm vacuum gap from 12Kh18N10T steel plates (Fig. 1b). The space in front of the free surface was also evacuated to a residual pressure of $P_{\text{res}} = 1.2$ kPa.

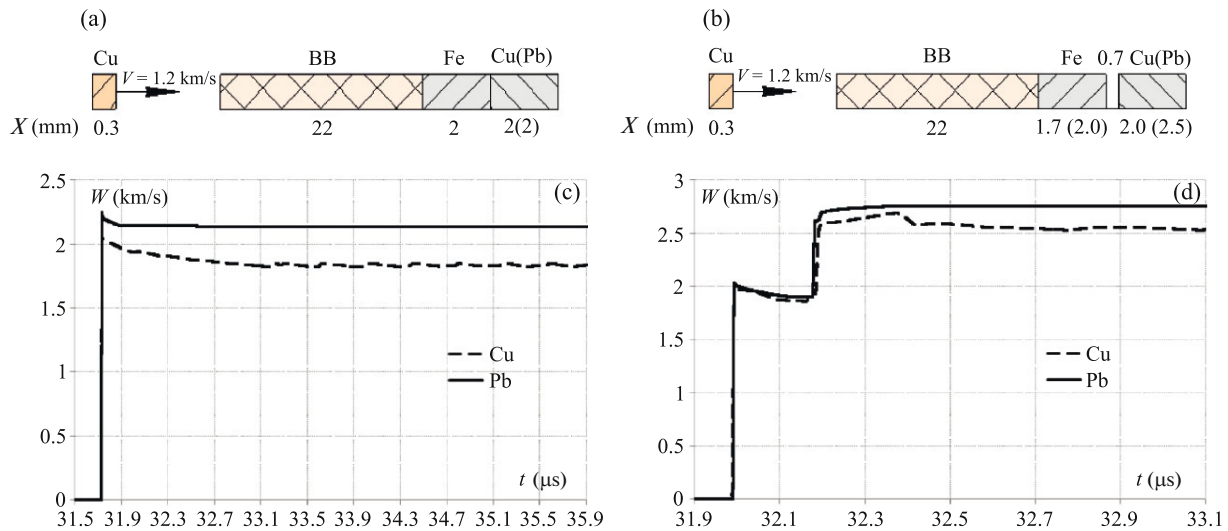


Fig. 1. (Color online) (a, b) Schematics of loading of the samples and (c, d) velocity profiles $W(t)$ for the incidence of (a, c) one and (b, d) two shock waves on the free surface.

Figures 1c and 1d present the time dependences of the velocity of the free surface calculated using one-dimensional programs developed at the Russian Federal Nuclear Center All-Russian Scientific Research Institute of Experimental Physics [26] for the one- and two-shock loading of the free surface of copper and lead liners.

The two-shock loading of the free surface is related to the circulation of shock waves and the rarefaction waves in copper (or lead) samples after the closure of the vacuum gap. The chosen loading schemes allow us to reach close velocities and pressure amplitudes under the incidence of the first and second shock waves on the free surface of the copper and lead samples and the time delay between waves of about $0.2 \mu\text{s}$. Copper does not melt under these loading conditions ($P_1 = 46$ GPa, $P_2 = 67$ GPa), whereas lead melts already on the first shock wave ($P_1 = 39$ GPa, $P_2 = 59$ GPa) [13, 19, 25]. These features are important for the study of shock-induced dusting. As in [23], the 2-mm-thick copper and lead samples 108 mm diameter were fabricated with a specially processed free surface whose 0.4-mm-thick stripe has the same roughness Rz20 ($2\alpha_0 = 20 \mu\text{m}$, $\lambda = 150 \mu\text{m}$).

To increase the informativeness and reliability of results, we simultaneously used shadow laser optical, X-ray diffraction, piezoelectric, and heterodyne interferometry (PDV sensors) methods for measurements.

Experiments were carried out at the Pylenie measuring-testing complex [17]. A qualitative picture and the quantitative characteristics of shock-induced dusting such as the velocities of the free surface and the particle flux front, as well as the density and mass distributions of the particle flux in the direction of its

motion, were obtained in each experimental with the listed methods. The experimental procedure was described in more detail in [23].

3. EXPERIMENTAL RESULTS AND THEIR DISCUSSION

The results obtained in this work using shadow laser optical recording and PDV sensors are presented in Figs. 2 and 3 in comparison with the results obtained in experiments with the incidence of one shock wave on the free surface (FS) [23]. These methods ensure the clearest visualization of the qualitative picture of dusting induced by one or two shock waves.

In particular, a particle flux noticeably ahead of the free surface and spall fragments near it are observed on shadow laser optical images in the case of the incidence of one shock wave on the free surface of the copper sample (Fig. 2b). In the case of the incidence of two successive shock waves on the free surface of a similar sample, the qualitative picture remains the same, but particles and spall fragments are entrained by the free surface accelerated by the second shock wave (Fig. 2d).

The qualitative picture of dusting induced by one shock wave incident on the free surface of the lead sample is noticeably different (Fig. 3a) apparently because of its melting. Cumulative jet flows are ejected from the microrelief on the free surface and then decay into particles under the action of the velocity gradient along the jets. As in the case of the copper samples, the second shock wave incident on the free surface of the lead sample compresses the particle flux (Fig. 3c).

The spectrograms of velocity profiles of the free surface and dust fluxes in the case of the incidence of one (Figs. 2b, 3b) or two (Figs. 2d, 3d) shock waves are

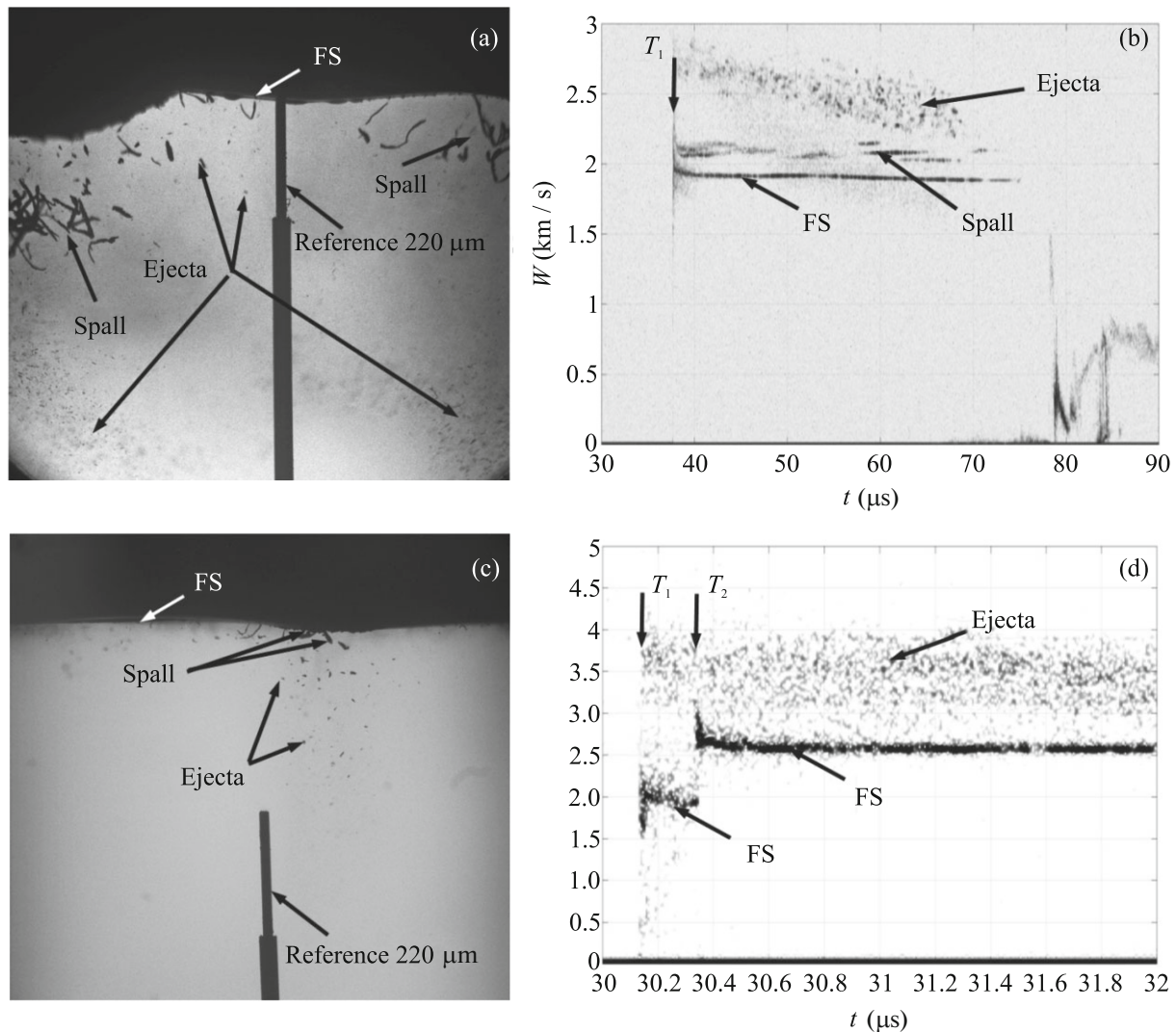


Fig. 2. Results of experiments for copper samples with the free surface exposed to (a, b) one and (c, d) two shock waves; T_1 and T_2 are the times of incidence of the first and second shock waves, respectively.

consistent with the qualitative picture of shock-induced dusting detected by shadow laser optical recording (Figs. 2a, 2c, 3a, and 3c). In particular, the spectrogram for the copper liner whose free surface is exposed to one shock wave exhibits features associated with the presence of particles and spall fragments in front of the free surface. The ejection of only particles is observed in the case of the incidence of two shock waves on the free surface of the copper liner, which are clearly detected at the times T_1 and T_2 . According to Fig. 2d, the velocity of the free surface after the incidence of the second shock wave increases from 2.0 to 2.7 km/s, whereas the velocity of the particle flux front $W_{FP} \approx 3.8$ km/s does not change. This can indicate that the second shock wave incident on the free surface does not induce additional ejection of particles. In the case of the incidence of one shock wave on the free surface of lead liners, the spectrogram demonstrates

features associated only with the presence of particles in front of the free surface. In the case of the incidence of two shock waves on the free surface of lead liners, the ejection of particles on the first shock wave ($W_{FP} \approx 2.8$ km/s) and the second shock wave ($W_{FP} \approx 3.6$ km/s) is observed at times T_1 and T_2 , respectively.

Figure 4 presents $X-t$ diagrams of the motion of the free surface and the leading edge of particle fluxes obtained with the data of all used methods, which demonstrate that they are in satisfactory agreement.

To determine the quantitative characteristics of mass fluxes of particles ejected under the incidence of two shock waves on the free surface, it is necessary to use quantitative X-ray diffraction (Figs. 5a, 5c) and piezoelectric (Figs. 5b, 5d) data obtained in these experiments. To reconstruct the density (mass) distribution in the particle flux (Fig. 6), reference copper

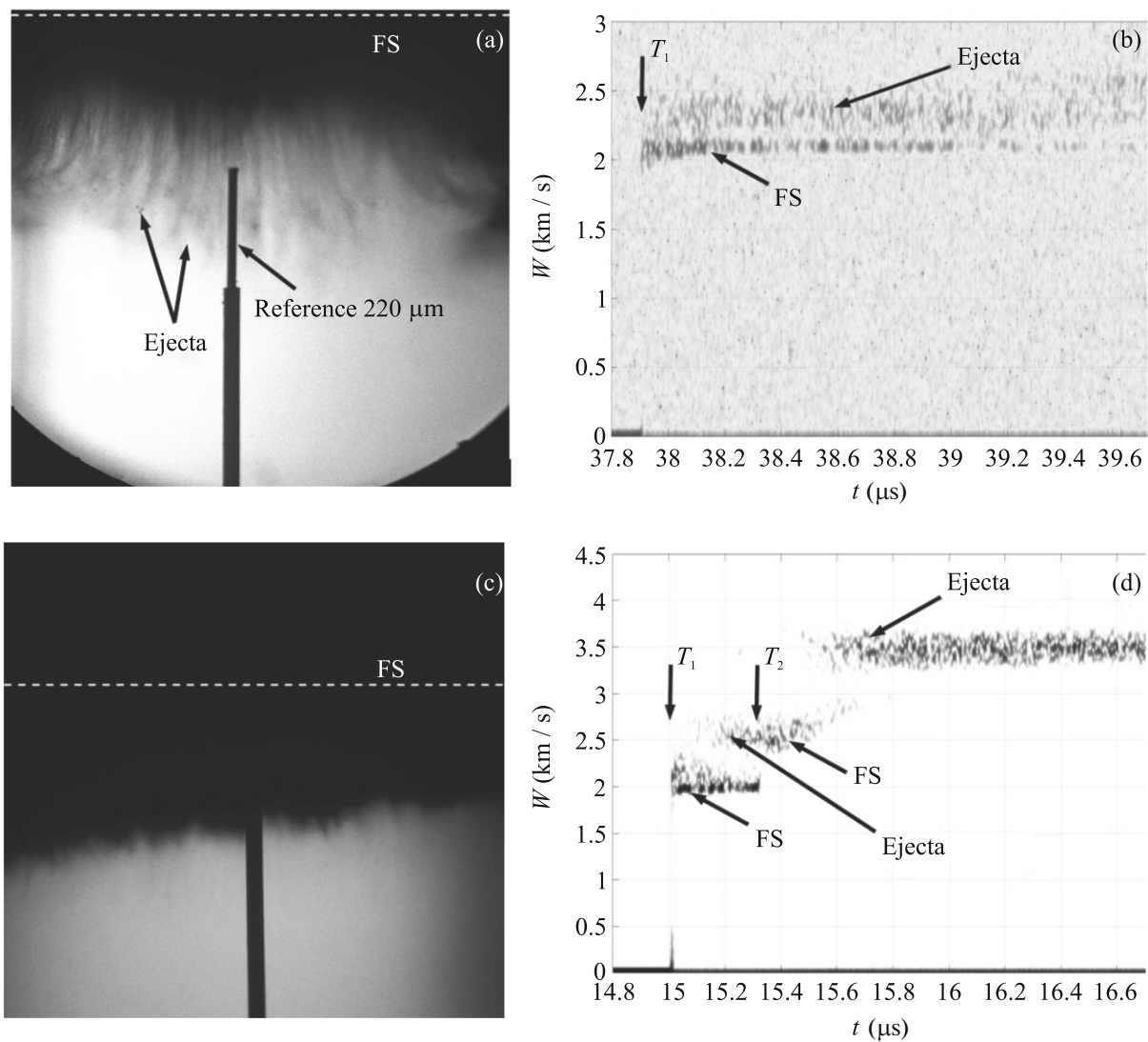


Fig. 3. Results of experiments for lead samples with the free surface exposed to (a, b) one and (c, d) two shock waves; T_1 and T_2 are the times of incidence of the first and second shock waves, respectively.

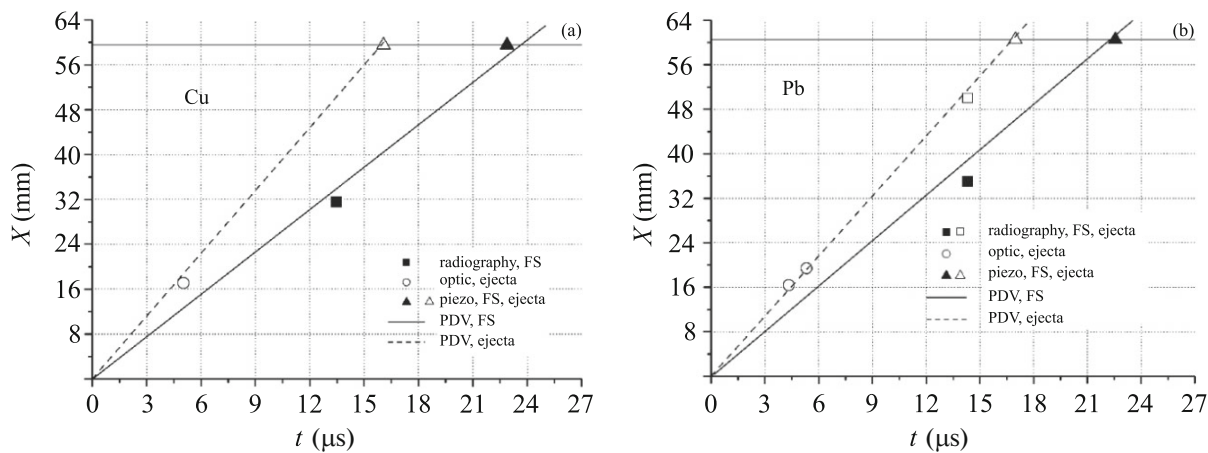


Fig. 4. $X-t$ diagrams of dusting from the free surface of the (a) copper and (b) lead samples exposed to two shock waves.

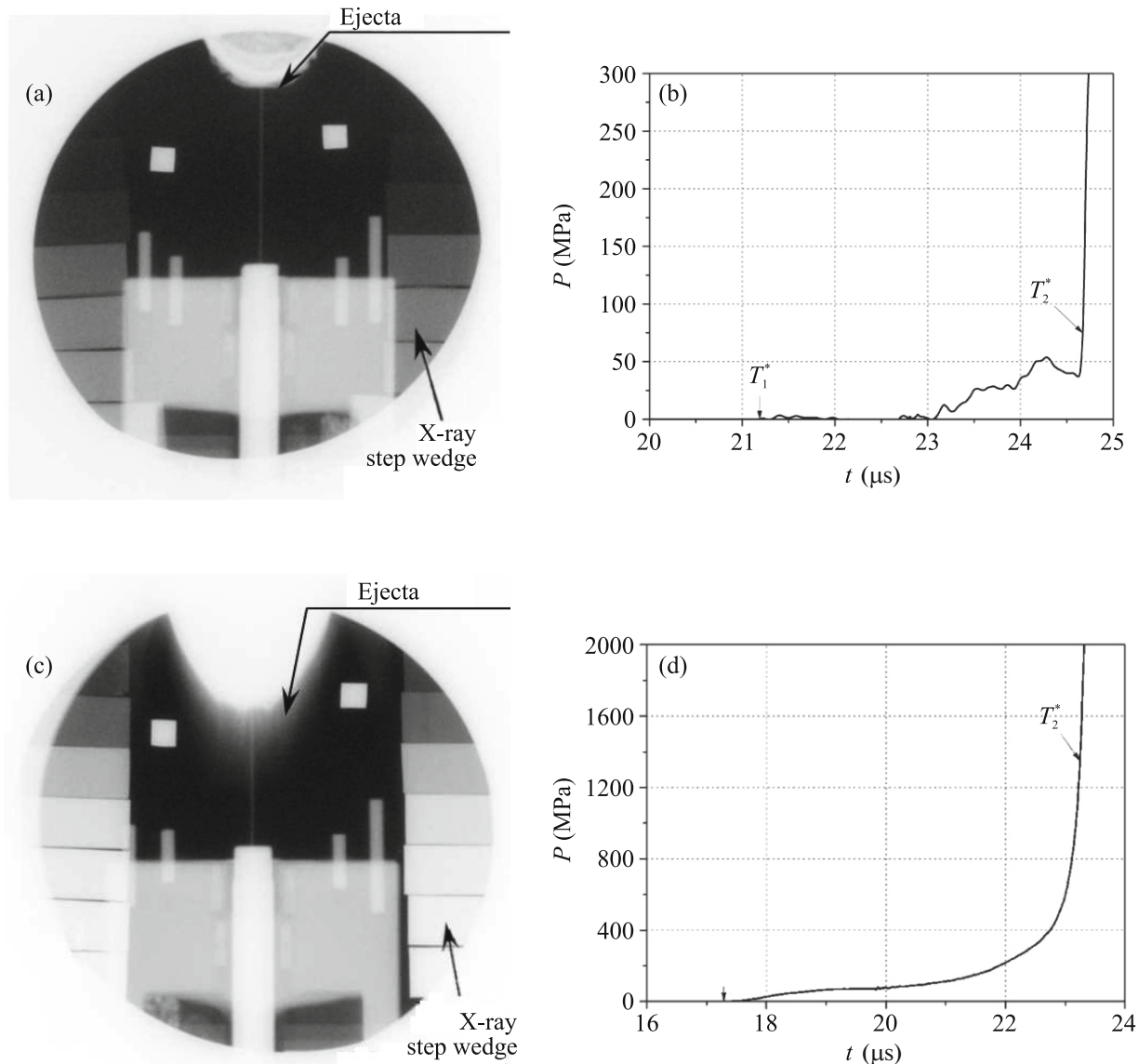


Fig. 5. (a, c) X-ray diffraction patterns and (b, d) pressure profiles obtained under the incidence of two shock waves on the free surface of the (a, b) copper and (c, d) lead liners; T_1^* and T_2^* are the times of arrival of the particle flux and the free surface at the piezoelectric sensors.

and lead wedges were used to transfer the darkening count matrix from the images in Figs. 5a and 5c to the mass thickness matrix, respectively [27].

Figure 6 presents the (a) density and (b) mass distributions in the particle flux in the direction of its propagation as functions of the (a) time and (b) relative velocity of particles in the flux reconstructed from X-ray diffraction and piezoelectric data. The masses of particle fluxes were determined for particles having velocities a factor of 1.05 higher than the velocity of the free surface. The density distribution in the particle flux from the copper liners was not reconstructed from

X-ray diffraction data because it is below the resolution of this method ($\rho_{\min}\Delta l = 1 \text{ mg/cm}^2$).

The averaged results of their processing in the same manner as in [23] are summarized in Table 1 in the form of the mass of the particle flux per unit surface.

Agreement between the mass distributions of fluxes depending on the relative velocity reconstructed using both methods is satisfactory. The analysis of the results indicates that the second shock wave incident on the free surface of copper liners, which do not melt under the experimental condition, apparently does not induce an additional ejection of particles, and the free surface accelerated by the second shock wave entrains

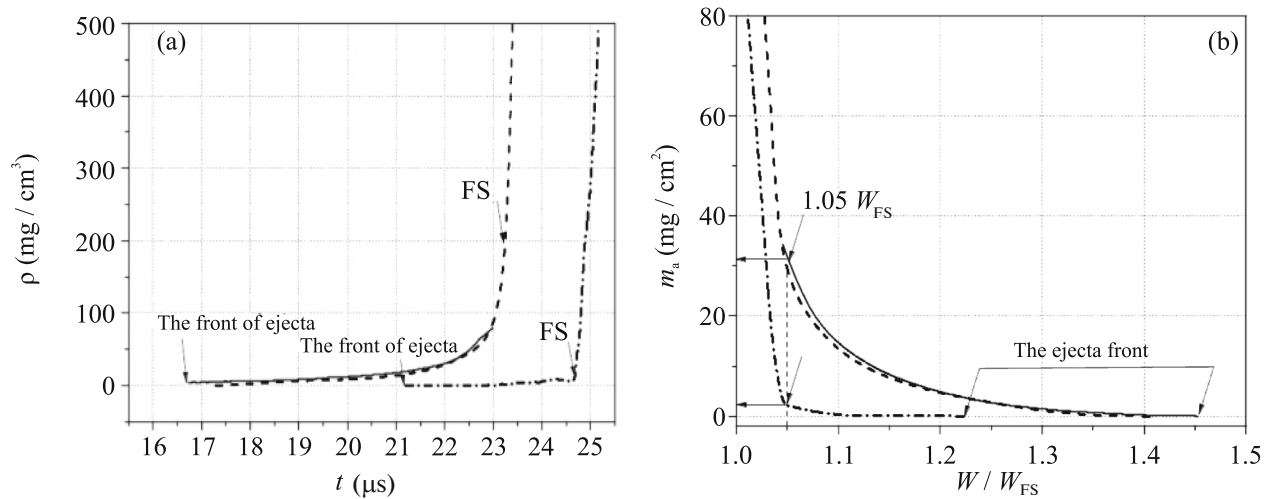


Fig. 6. (a) Density and (b) mass distributions in the particle flux in the direction of its motion versus (a) the time and (b) the relative velocity of particles in the flux in lead according to (solid lines) X-ray diffraction data and (dashed lines) piezoelectric data and (dash-dotted lines) in copper according to piezoelectric data.

slower particles formed under the incidence of the first shock wave. Therefore, the mass of the particle flux after the incidence of two shock waves on the free surface is noticeably smaller than that in the case of the incidence of one shock wave (Table 1). The masses of the particle flux from the lead liners, which melt after the incidence of the first shock wave on the free surface, after the incidence of one and two shock waves on the free surface are close to each other. This relation can be due to the fact that the second shock wave induces an additional ejection of particles from the regions between jets and accelerates the free surface that entrains larger and slower particles, which reduces the total number of particles in the flux. As a result, the masses of particle fluxes in the case of one and two shock waves incident on lead liners, which melt under these loading conditions, are close to each other.

4. CONCLUSIONS

The study of particle ejection from the free surface of the samples with the roughness Rz20 exposed to

Table 1. Averaged particle flux masses per unit surface measured by X-ray diffraction and piezoelectric methods

Material	Number of shock waves	Roughness $2\alpha/\lambda$, μm	m , mg/cm ²
Copper	1 [23]	20/150	12.5 ± 1.9
	2	15/150	0.7 ± 0.3
Lead	1 [23]	18/150	25.0 ± 3.8
	2	20/120	26.5 ± 4.0

two successive shock waves with amplitudes of 46 and 67 GPa (for copper) and 39 and 59 GPa (for lead) separated in time by ~ 0.2 – 0.3 μs gives the following results.

- The qualitative picture of shock-induced dusting, as well as in the case of the incidence of one shock wave, is determined by the strength or the phase state of the material and is characterized by the ejection of the particle flux and micro-spall fragments if the material (copper) does not melt and by the ejection of jet flows with their subsequent decay into micro-particles if the material (lead) melts under shock compression.

- The incidence of the second shock wave on the free surface results in the additional particle ejection if the material of the liner has a low strength (lead melts) and does not lead to a noticeable additional particle ejection if the material has a high strength (copper does not melt).

- The velocities of the particle flux front from copper and lead liners are 3.8 and 3.6 km/s, respectively, and are determined by the incidence of the first and second shock waves on the free surface, respectively.

- The particle flux mass per unit surface decreases from (12.5 ± 1.5) mg/cm² to (0.7 ± 0.3) mg/cm² for copper liners because of the capture of ejected spall fragments and particles from the free surface accelerated by the second shock wave and keeps an almost unchanged value of (26.0 ± 4.0) mg/cm² for lead liners because of the additional ejection of particles on the second shock wave and capture of slower particles from the free surface.

FUNDING

This study was supported by the Russian Science Foundation, project no. 23-22-00051, <https://rscf.ru/project/23-22-00051/>.

CONFLICT OF INTEREST

The authors declare that they have no conflicts of interest.

OPEN ACCESS

This article is licensed under a Creative Commons Attribution 4.0 International License, which permits use, sharing, adaptation, distribution and reproduction in any medium or format, as long as you give appropriate credit to the original author(s) and the source, provide a link to the Creative Commons license, and indicate if changes were made. The images or other third party material in this article are included in the article’s Creative Commons license, unless indicated otherwise in a credit line to the material. If material is not included in the article’s Creative Commons license and your intended use is not permitted by statutory regulation or exceeds the permitted use, you will need to obtain permission directly from the copyright holder. To view a copy of this license, visit <http://creativecommons.org/licenses/by/4.0/>.

REFERENCES

1. V. A. Ogorodnikov, A. L. Mikhailov, V. V. Burtsev, S. A. Lobastov, S. V. Erunov, A. V. Romanov, A. V. Rudnev, E. V. Kulakov, Yu. B. Bazarov, V. V. Glushikhin, I. A. Kalashnik, V. A. Tsyganov, and B. I. Tkachenko, *J. Exp. Theor. Phys.* **109**, 530 (2009).
2. S. B. Bakhrakh, I. Yu. Bezrukova, A. D. Kovaleva, S. S. Kosarin, and O. V. Ol’khov, *Vopr. At. Nauki Tekh., Ser.: Mat. Model. Fiz. Protsess., No. 3*, 14 (2005).
3. T. de Resseguier, L. Signor, A. Dragon, M. Boustie, G. Roy, and F. Llorca, *J. Appl. Phys.* **101**, 013506 (2007).
4. M. B. Zellner, M. Grover, J. E. Hammerberg, et al., *J. Appl. Phys.* **102**, 013522 (2007).
5. T. C. Germann, J. E. Hammerber, and G. Dimonte, in *Proceedings of the 7th Biannual International Conference on New Models and Hydrocodes for Shock Wave Processes in Condensed Matter, Portugal, Estorie May 18–23, 2008* (ADAI, Lisbon, 2008).
6. N. V. Nevmerzhitskii, A. L. Mikhailov, V. A. Raevskii, V. S. Sasik, Yu. M. Makarov, E. A. Sotskov, and A. V. Rudnev, in *Proceedings of the 13th International Conference Kharitonov Readings* (RFYaTs-VNIIEF, Sarov, 2011), p. 604.
7. A. B. Georgievskaya and V. A. Raevskii, in *Proceedings of the 13th International Conference Kharitonov Readings* (RFYaTs-VNIIEF, Sarov, 2011), p. 597.
8. G. Dimonte, G. Terrones, and F. Cherne, *Phys. Rev. Lett.* **107**, 264502 (2011).
9. Y. Chen, H. Hu, T. Tang, G. Ren, and Q. Li, *J. Appl. Phys.* **111**, 053509 (2012).
10. D. M. Or’o, J. E. Hammerberg, W. T. Buttler, F. G. Mariam, C. Morris, C. Rousculp, and J. B. Stone, *AIP Conf. Proc.* **1426**, 1351 (2012).
11. D. S. Sorenson, R. M. Malone, G. A. Capelle, P. Pazu-chanics, R. P. Johnson, M. L. Kaufman, A. Tibbitts, T. Tunnell, D. Marks, M. Grover, B. Marshall, G. D. Stevens, W. D. Turley, and B. LaLone, in *Proceedings of the NEDPC 2013, Livermore, CA*, LA-UR-14-23036 (2013).
12. M. V. Antipov, A. B. Georgievskaya, V. V. Igonin, V. N. Knyazev, A. I. Lebedev, M. O. Lebedeva, K. N. Pano, V. A. Raevskii, V. D. Sadunov, A. A. Utenkov, and I. V. Yurtov, in *Proceedings of the 15th International Conference Kharitonov Readings* (RFYaTs-VNIIEF, Sarov, 2013), p. 666.
13. A. V. Fedorov, A. L. Mikhailov, S. A. Finyushin, D. V. Nazarov, E. A. Chudakov, D. A. Kalashnikov, and E. I. Butusov, in *Proceedings of the 15th International Conference Kharitonov Readings* (RFYaTs-VNIIEF, Sarov, 2013), p. 274.
14. N. V. Nevmerzhitskii, E. A. Sotskov, E. D. Sen’kovskii, S. A. Abakumov, S. V. Frolov, O. A. Krivonos, A. V. Rudnev, O. N. Aprelkov, and A. B. Georgievskaya, in *Proceedings of the 15th International Conference Kharitonov Readings* (RFYaTs-VNIIEF, Sarov, 2013), p. 655.
15. S. K. Monfared, D. M. Or’o, M. Grover, J. E. Hammerberg, B. M. LaLone, C. L. Pack, M. M. Schauer, G. D. Stevens, J. B. Stone, W. D. Turley, and W. T. Buttler, *J. Appl. Phys.* **116**, 063504 (2014).
16. S. K. Monfared, W. T. Buttler, D. K. Frayer, M. Grover, J. E. Hammerberg, B. M. LaLone, G. D. Stevens, J. B. Stone, W. D. Turley, and M. M. Schauer, *J. Appl. Phys.* **117**, 223105 (2015).
17. A. L. Mikhailov, V. A. Ogorodnikov, V. S. Sasik, V. A. Raevskii, A. I. Lebedev, D. E. Zotov, S. V. Erunov, M. A. Syrunin, V. D. Sadunov, N. V. Nevmerzhitskii, S. A. Lobastov, V. V. Burtsev, A. V. Mishanov, E. V. Kulakov, A. V. Satarova, et al., *J. Exp. Theor. Phys.* **118**, 785 (2014).
18. V. A. Ogorodnikov, A. L. Mikhailov, V. S. Sasik, S. V. Erunov, M. A. Syrunin, A. V. Fedorov, N. V. Nevmerzhitskii, E. V. Kulakov, O. A. Kleshchevnikov, M. V. Antipov, I. V. Yurtov, A. V. Rudnev, A. V. Chapaev, A. S. Pupkov, E. D. Sen’kovskii, et al., *J. Exp. Theor. Phys.* **122**, 357 (2016).
19. V. A. Ogorodnikov, A. L. Mikhailov, S. V. Erunov, M. V. Antipov, A. V. Fedorov, M. A. Syrunin, E. V. Kulakov, O. A. Kleshchevnikov, I. V. Yurtov, A. A. Utenkov, S. A. Finyushin, E. A. Chudakov, D. A. Kalashnikov, A. S. Pupkov, A. V. Chapaev, et al., *J. Exp. Theor. Phys.* **125**, 985 (2017).
20. W. T. Buttler, S. K. Lamoreaux, R. K. Schulze, et al., *J. Dyn. Behav. Mater.* **3**, 334 (2017).
21. V. A. Ogorodnikov, A. L. Mikhaylov, S. V. Erunov, et al., *J. Dyn. Behav. Mater.* **3**, 225 (2017).
22. N. V. Nevmerzhitskii, V. A. Raevskii, E. A. Sotskov, E. D. Sen’kovskii, N. B. Davydov, E. V. Bodrov, S. V. Frolov, K. V. Anisiforov, A. B. Georgievskaya, E. V. Levkina, O. L. Krivonos, A. S. Kuchkareva, A. R. Gavrish, and B. I. Tkachenko, *Combust. Explos., Shock Waves* **54**, 585 (2018).

23. V. A. Ogorodnikov, A. L. Mikhailov, S. V. Erunov, S. A. Finyushin, D. E. Zotov, N. V. Nevmerzhitskii, A. I. Bystruev, M. A. Syrunin, M. V. Antipov, A. V. Fedorov, K. N. Panov, E. V. Kulakov, A. A. Utenkov, I. V. Yurtov, E. A. Chudakov, et al., *J. Exp. Theor. Phys.* **129**, 397 (2019).
24. V. A. Ogorodnikov, S. V. Erunov, A. O. Blikov, E. V. Kulakov, E. A. Chudakov, M. V. Antipov, K. N. Panov, M. A. Syrunin, V. N. Knyazev, N. B. Davydov, A. B. Georgievskaya, A. O. Yagovkin, I. V. Yurtov, D. N. Zamyslov, A. E. Kovalev, et al., *J. Exp. Theor. Phys.* **133**, 533 (2021).
25. V. P. Kopyshv and A. V. Medvedev, Preprint (RFYaTs-VNIIEF, Sarov, 1995).
26. N. F. Gavrilo, G. G. Ivanova, V. I. Semin, and V. N. Sofronov, *Vopr. At. Nauki Tekh., Ser. Metod. Programmy Chisl. Reshen. Zadach Mat. Fiz.*, No. 3, 11 (1982).
27. M. V. Antipov, A. B., Georgievskaya, V. V. Igonin, M. O. Lebedeva, K. N. Panov, A. A. Utenkov, V. D. Sadunov, and I. V. Yurtov, in *Proceedings of the 17th International Conference Kharitonov Readings* (RFYaTs-VNIIEF, Sarov, 2015), p. 702.

Translated by R. Tyapaev